HELMHOLTZ MUNICH

Computational Imaging and AI in Medicine

Helmholtz Munich, Institute of Machine Learning in Biomedical Imaging
Technical University of Munich, Institute for Computational Imaging and AI in Medicine

Daniel Lang
lang@helmholtz-munich.de

Medical Imaging

Modalities:

- computed tomography (CT)
- magnetic resonance imaging (MRI)

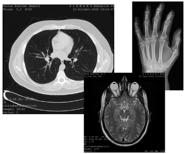

HELMHOLTZ MUNICH

Medical Imaging

Modalities:

- computed tomography (CT)
- magnetic resonance imaging (MRI)
- x-ray, ultrasound, SPECT, PET

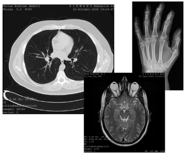

Medical Imaging

Modalities:

- computed tomography (CT)
- magnetic resonance imaging (MRI)
- x-ray, ultrasound, SPECT, PET

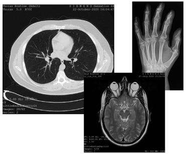

Tasks:

- reconstruction/motion correction

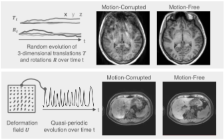

HELMHOLTZ MUNICH

Medical Imaging

Modalities:

- computed tomography (CT)
- magnetic resonance imaging (MRI)
- x-ray, ultrasound, SPECT, PET

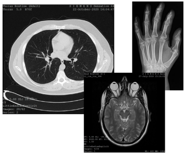

Tasks:

- reconstruction/motion correction
  - acquired/filtered in frequency space
  - motion between slices

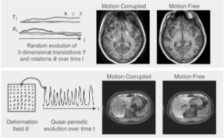

Medical Imaging

Modalities:

- computed tomography (CT)
- magnetic resonance imaging (MRI)
- x-ray, ultrasound, SPECT, PET

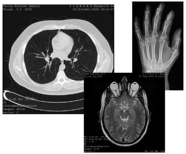

Tasks:

- reconstruction/motion correction
- registration

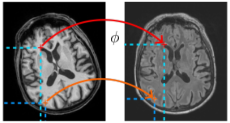

Medical Imaging

Modalities:

- computed tomography (CT)
- magnetic resonance imaging (MRI)
- x-ray, ultrasound, SPECT, PET

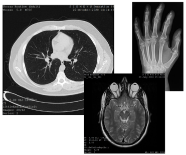

Tasks:

- reconstruction/motion correction
- registration
  - images from different time-points

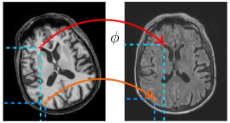

HELMHOLTZ MUNICH

Medical Imaging

Modalities:

- computed tomography (CT)
- magnetic resonance imaging (MRI)
- x-ray, ultrasound, SPECT, PET

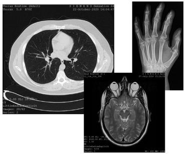

Tasks:

- reconstruction/motion correction
- registration
- image segmentation

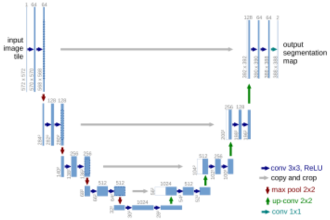

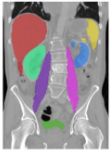

Medical Imaging

Modalities:

- computed tomography (CT)
- magnetic resonance imaging (MRI)
- x-ray, ultrasound, SPECT, PET

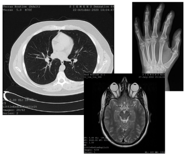

Tasks:

- reconstruction/motion correction
- registration
- image segmentation
  - identification of region of interests and organs of risk

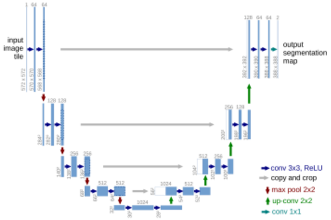

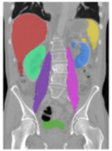

Medical Imaging

Modalities:

- computed tomography (CT)
- magnetic resonance imaging (MRI)
- x-ray, ultrasound, SPECT, PET

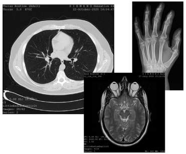

Tasks:

- reconstruction/motion correction
- registration
- image segmentation
- detection/classification

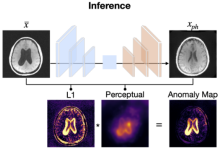

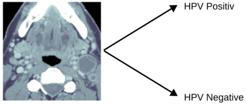

HELMHOLTZ MUNICH

Medical Imaging

Modalities:

- computed tomography (CT)
- magnetic resonance imaging (MRI)
- x-ray, ultrasound, SPECT, PET

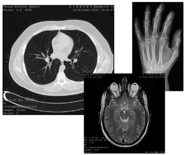

Tasks:

- reconstruction/motion correction
- registration
- image segmentation
- detection/classification
  - replacement of invasive testing
  - development of novel markers, e.g. survival

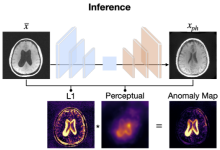

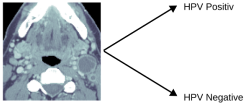

Oropharynx Cancer

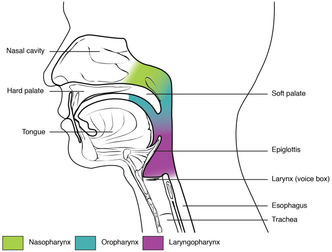

- "classically" driven by smoking and alcohol consumption
- cases driven by the human papillomavirus (HPV) on the rise
  - more radiosensitive[1]

- biopsy for HPV testing
- only 2/3 tested in north America[2]

[1] "The molecular mechanisms of increased radiosensitivity of HPV-positive OPSCC", Liu et al., 2018

[2] "North-American survey on HPV-DNA and p16 testing for head and neck squamous cell carcinoma", Maniakas et al., 2014

HELMHOLTZ MUNICH

Oropharynx Cancer

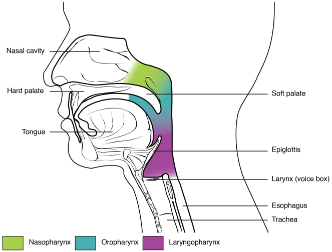

- "classically" driven by smoking and alcohol consumption
- cases driven by the human papillomavirus (HPV) on the rise
  - more radiosensitive[1]

- biopsy for HPV testing
- only 2/3 tested in north America[2]

Can we train a algorithm to classify HPV based on CT images?

---

[1] "The molecular mechanisms of increased radiosensitivity of HPV-positive OPSCC", Liu et al., 2018

[2] "North-American survey on HPV-DNA and p16 testing for head and neck squamous cell carcinoma", Maniakas et al., 2014

Data

- diverse data set (external testing)

	training set		validation set	test set
	OPC	**HNSCC**	**HN PET-CT**	**HN1**
Patients	412	263	90	80
HPV: pos/neg	290/122	223/40	71/19	23/57
HPV status				
Age				
pos	58.81 (52.00-64.75)	57.87 (52.00-64.00)	62.32 (58.00-66.00)	57.52 (52.00-62.50)
neg	64.82 (58.00-72.75)	60.02 (54.50-67.25)	59.11 (49.50-69.50)	60.91 (56.00-66.00)
Sex: Female/Male				
pos	47/243	32/191	14/56	5/18
neg	34/88	15/25	4/15	12/45
T-stage: T1/T2/T3/T4				
pos	46/93/94/57	60/93/41/29	10/37/15/9	4/8/9/8
neg	9/35/43/35	6/12/12/10	3/4/8/4	9/16/9/23
N-stage: N0/N1/N2/N3				
pos	33/22/215/20	19/30/170/4	11/10/47/3	6/2/15/0
neg	36/16/62/8	5/2/31/2	2/1/13/3	14/10/31/2
Tumor size [cm^3]				
pos	29.35 (10.52-37.78)	11.78 (3.94-14.04)	34.63 (14.91-41.77)	23.00 (10.83-34.29)
neg	36.99 (15.72-45.35)	23.57 (5.80-22.85)	35.09 (17.32-47.82)	40.19 (11.77-54.42)
transversal voxel spacing [mm]	0.97 (0.98-0.98)	0.59 (0.49-0.51)	1.06 (0.98-1.17)	0.98 (0.98-0.98)
longitudinal voxel spacing [mm]	2.00 (2.00-2.00)	1.53 (1.00-2.50)	2.89 (3.00-3.27)	2.99 (3.00-3.00)
manufacturer				
GE Med. Sys.	272	238	45	0
Toshiba	138	3	0	0
Philips	2	12	45	0
CMS Inc.	0	0	0	43
Siemens	0	4	0	37
other	0	6	0	0

Data

- diverse data set (external testing)

	training set		validation set	test set
	OPC	**HNSCC**	**HN PET-CT**	**HN1**
Patients	412	263	90	80
HPV: pos/neg	290/122	223/40	71/19	23/57
HPV status				
Age				
pos	58.81 (52.00-64.75)	57.87 (52.00-64.00)	62.32 (58.00-66.00)	57.52 (52.00-62.50)
neg	64.82 (58.00-72.75)	60.02 (54.50-67.25)	59.11 (49.50-69.50)	60.91 (56.00-66.00)
Sex: Female/Male				
pos	47/243	32/191	14/56	5/18
neg	34/88	15/25	4/15	12/45
T-stage: T1/T2/T3/T4				
pos	46/93/94/57	60/93/41/29	10/37/15/9	4/8/9/8
neg	9/35/43/35	6/12/12/10	3/4/8/4	9/16/9/23
N-stage: N0/N1/N2/N3				
pos	33/22/215/20	19/30/170/4	11/10/47/3	6/2/15/0
neg	36/16/62/8	5/2/31/2	2/1/13/3	14/10/31/2
Tumor size [cm^3]				
pos	29.35 (10.52-37.78)	11.78 (3.94-14.04)	34.63 (14.91-41.77)	23.00 (10.83-34.29)
neg	36.99 (15.72-45.35)	23.57 (5.80-22.85)	35.09 (17.32-47.82)	40.19 (11.77-54.42)
transversal voxel spacing [mm]	0.97 (0.98-0.98)	0.59 (0.49-0.51)	1.06 (0.98-1.17)	0.98 (0.98-0.98)
longitudinal voxel spacing [mm]	2.00 (2.00-2.00)	1.53 (1.00-2.50)	2.89 (3.00-3.27)	2.99 (3.00-3.00)
manufacturer				
GE Med. Sys.	272	238	45	0
Toshiba	138	3	0	0
Philips	2	12	45	0
CMS Inc.	0	0	0	43
Siemens	0	4	0	37
other	0	6	0	0

- still very small (in terms of deep learning)

HELMHOLTZ MUNICH

Data

- diverse data set (external testing)

	training set		validation set	test set
	OPC	**HNSCC**	**HN PET-CT**	**HN1**
Patients	412	263	90	80
HPV: pos/neg	290/122	223/40	71/19	23/57
HPV status				
Age				
pos	58.81 (52.00-64.75)	57.87 (52.00-64.00)	62.32 (58.00-66.00)	57.52 (52.00-62.50)
neg	64.82 (58.00-72.75)	60.02 (54.50-67.25)	59.11 (49.50-69.50)	60.91 (56.00-66.00)
Sex: Female/Male				
pos	47/243	32/191	14/56	5/18
neg	34/88	15/25	4/15	12/45
T-stage: T1/T2/T3/T4				
pos	46/93/94/57	60/93/41/29	10/37/15/9	4/8/9/8
neg	9/35/43/35	6/12/12/10	3/4/8/4	9/16/9/23
N-stage: N0/N1/N2/N3				
pos	33/22/215/20	19/30/170/4	11/10/47/3	6/2/15/0
neg	36/16/62/8	5/2/31/2	2/1/13/3	14/10/31/2
Tumor size [cm^3]				
pos	29.35 (10.52-37.78)	11.78 (3.94-14.04)	34.63 (14.91-41.77)	23.00 (10.83-34.29)
neg	36.99 (15.72-45.35)	23.57 (5.80-22.85)	35.09 (17.32-47.82)	40.19 (11.77-54.42)
transversal voxel spacing [mm]	0.97 (0.98-0.98)	0.59 (0.49-0.51)	1.06 (0.98-1.17)	0.98 (0.98-0.98)
longitudinal voxel spacing [mm]	2.00 (2.00-2.00)	1.53 (1.00-2.50)	2.89 (3.00-3.27)	2.99 (3.00-3.00)
manufacturer				
GE Med. Sys.	272	238	45	0
Toshiba	138	3	0	0
Philips	2	12	45	0
CMS Inc.	0	0	0	43
Siemens	0	4	0	37
other	0	6	0	0

- still very small (in terms of deep learning)

  $\rightarrow$ transfer learning

  knowledge gained from initial task P_1 *to improve downstream task* P_2

Data

- diverse data set (external testing)

	training set		validation set	test set
	OPC	**HNSCC**	**HN PET-CT**	**HN1**
Patients	412	263	90	80
HPV: pos/neg	290/122	223/40	71/19	23/57
HPV status				
Age				
pos	58.81 (52.00-64.75)	57.87 (52.00-64.00)	62.32 (58.00-66.00)	57.52 (52.00-62.50)
neg	64.82 (58.00-72.75)	60.02 (54.50-67.25)	59.11 (49.50-69.50)	60.91 (56.00-66.00)
Sex: Female/Male				
pos	47/243	32/191	14/56	5/18
neg	34/88	15/25	4/15	12/45
T-stage: T1/T2/T3/T4				
pos	46/93/94/57	60/93/41/29	10/37/15/9	4/8/9/8
neg	9/35/43/35	6/12/12/10	3/4/8/4	9/16/9/23
N-stage: N0/N1/N2/N3				
pos	33/22/215/20	19/30/170/4	11/10/47/3	6/2/15/0
neg	36/16/62/8	5/2/31/2	2/1/13/3	14/10/31/2
Tumor size [cm^3]				
pos	29.35 (10.52-37.78)	11.78 (3.94-14.04)	34.63 (14.91-41.77)	23.00 (10.83-34.29)
neg	36.99 (15.72-45.35)	23.57 (5.80-22.85)	35.09 (17.32-47.82)	40.19 (11.77-54.42)
transversal voxel spacing [mm]	0.97 (0.98-0.98)	0.59 (0.49-0.51)	1.06 (0.98-1.17)	0.98 (0.98-0.98)
longitudinal voxel spacing [mm]	2.00 (2.00-2.00)	1.53 (1.00-2.50)	2.89 (3.00-3.27)	2.99 (3.00-3.00)
manufacturer				
GE Med. Sys.	272	238	45	0
Toshiba	138	3	0	0
Philips	2	12	45	0
CMS Inc.	0	0	0	43
Siemens	0	4	0	37
other	0	6	0	0

- still very small (in terms of deep learning)

  $\rightarrow$ transfer learning

  knowledge gained from initial task P_1 *to improve downstream task* P_2

  but: CT data is 3D (models usually pretrained on ImageNet)

Learning Spatiotemporal Features with 3D Convolutional Networks

Du Tran[1,2], Lubomir Bourdev[1], Rob Fergus[1], Lorenzo Torresani[2], Manohar Paluri[1]
[1]Facebook AI Research, [2]Dartmouth College
{dutran,lorenzo}@cs.dartmouth.edu {lubomir,robfergus,mano}@fb.com

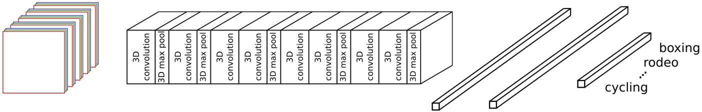

"Learning spatiotemporal features with 3d convolutional networks", Tran et al., 2015

Learning Spatiotemporal Features with 3D Convolutional Networks

Du Tran[1,2], Lubomir Bourdev[1], Rob Fergus[1], Lorenzo Torresani[2], Manohar Paluri[1]
[1]Facebook AI Research, [2]Dartmouth College
{dutran,lorenzo}@cs.dartmouth.edu {lubomir,robfergus,mano}@fb.com

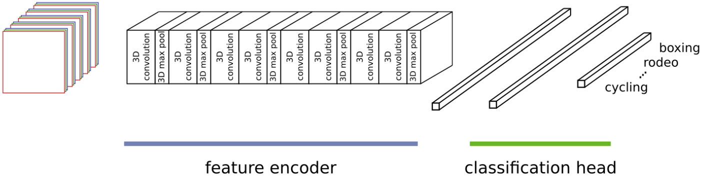

"Learning spatiotemporal features with 3d convolutional networks", Tran et al., 2015

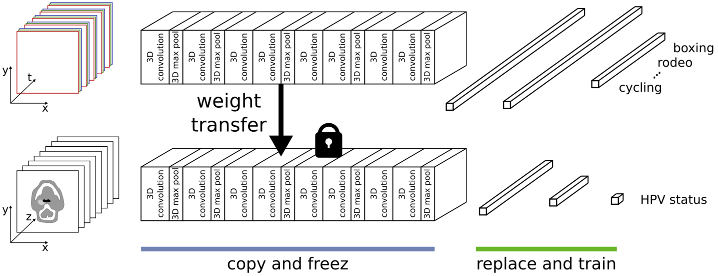

“Learning spatiotemporal features with 3d convolutional networks”, Tran et al., 2015

Results

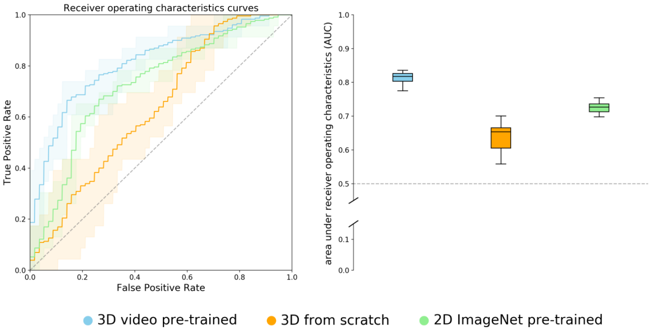

AUC	C3D	CNN	VGG
test set	0.81 (0.77, 0.84)	0.64 (0.56, 0.70)	0.73 (0.70, 0.75)

- AUC: probability that a randomly chosen case with a positive ground truth label is ranked with greater suspicion than a randomly chosen ground truth negative case

HELMHOLTZ MUNICH

"Deep learning based HPV status prediction for oropharyngeal cancer patients", Lang et al., 2021

Is there no better solution?

Is there no better solution? $\rightarrow$ Self-supervised Learning

Masked Autoencoders Are Scalable Vision Learners

Kaiming He[*,†] Xinlei Chen[*] Saining Xie Yanghao Li Piotr Dollár Ross Girshick

[*]equal technical contribution [†]project lead

Facebook AI Research (FAIR)

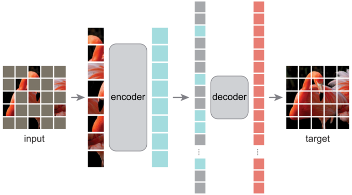

Masked Autoencoders Are Scalable Vision Learners

Kaiming He*,† Xinlei Chen* Saining Xie Yanghao Li Piotr Dollár Ross Girshick

*equal technical contribution †project lead

Facebook AI Research (FAIR)

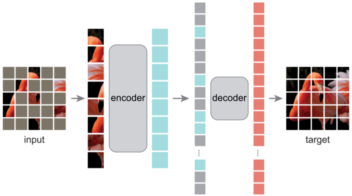

- masking for self-supervised pretraining
  - no need for labeled data

Masked Autoencoders Are Scalable Vision Learners

Kaiming He*,† Xinlei Chen* Saining Xie Yanghao Li Piotr Dollár Ross Girshick

*equal technical contribution †project lead

Facebook AI Research (FAIR)

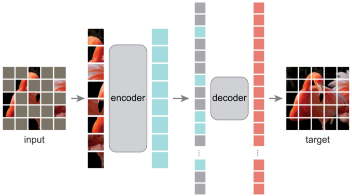

- masking for self-supervised pretraining
  - no need for labeled data
- transformer based autoencoder

HELMHOLTZ MUNICH

Masked Autoencoders Are Scalable Vision Learners

Kaiming He[*,†] Xinlei Chen[*] Saining Xie Yanghao Li Piotr Dollár Ross Girshick

[*]equal technical contribution [†]project lead

Facebook AI Research (FAIR)

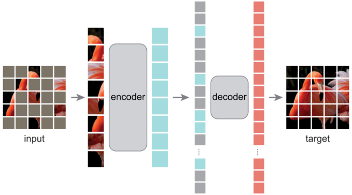

- masking for self-supervised pretraining
  - no need for labeled data
- transformer based autoencoder

Attention Is All You Need

Ashish Vaswani[*] Google Brain avaswani@google.com

Noam Shazeer[*] Google Brain noam@google.com

Niki Parmar[*] Google Research nikip@google.com

Jakob Uszkoreit[*] Google Research usz@google.com

Llion Jones[*] Google Research llion@google.com

Aidan N. Gomez[* †] University of Toronto aidan@cs.toronto.edu

Łukasz Kaiser[*] Google Brain lukaszkaiser@google.com

Illia Polosukhin[* ‡] illia.polosukhin@gmail.com

$$PE_{(pos,2i)} = sin(pos/10000^{2i/d_{\text{model}}})$$
$$PE_{(pos,2i+1)} = cos(pos/10000^{2i/d_{\text{model}}})$$

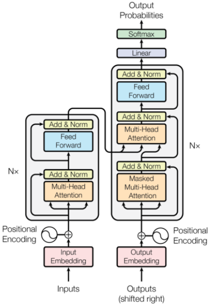

HELMHOLTZ MUNICH

Masked Autoencoders Are Scalable Vision Learners

Kaiming He[*,†] Xinlei Chen[*] Saining Xie Yanghao Li Piotr Dollár Ross Girshick

[*]equal technical contribution [†]project lead

Facebook AI Research (FAIR)

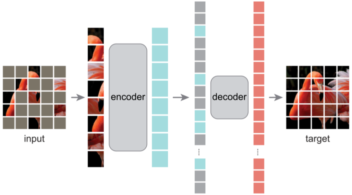

- masking for self-supervised pretraining
  - no need for labeled data
- transformer based autoencoder

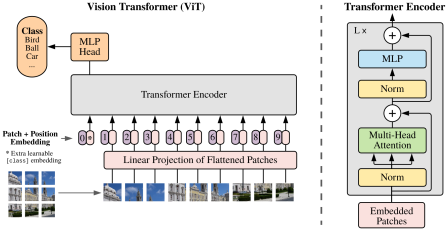

HELMHOLTZ MUNICH

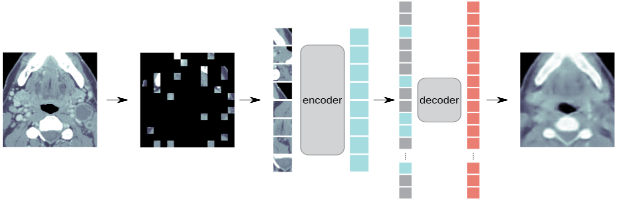
encoder
decoder

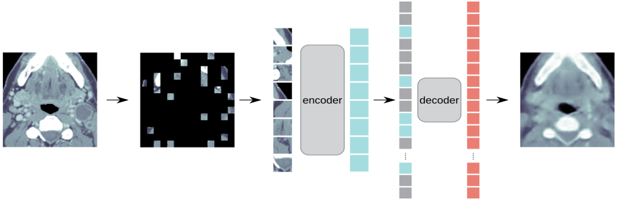

- mask the input for self-supervised pretraining
  - cases without HPV status

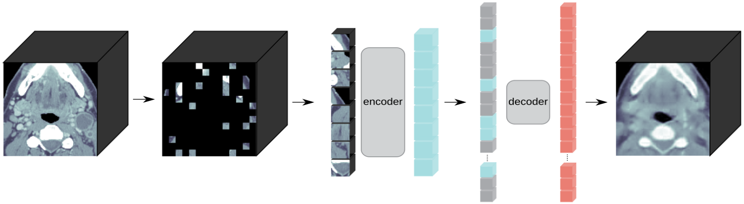

- mask the input for self-supervised pretraining
  - cases without HPV status
- remodel the vision transformer to be able to handle 3D data

HELMHOLTZ MUNICH

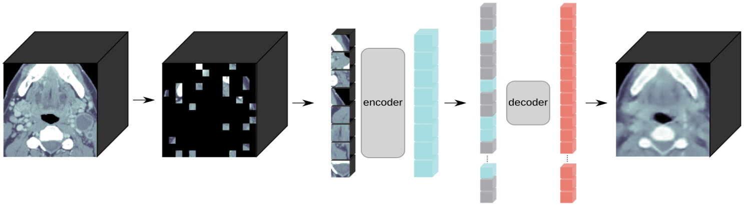

- mask the input for self-supervised pretraining
  - cases without HPV status
- remodel the vision transformer to be able to handle 3D data

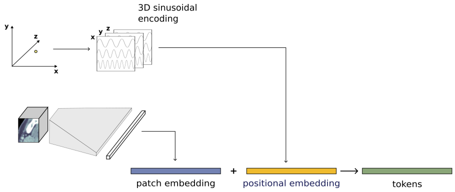

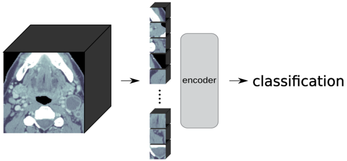

- mask the input for self-supervised pretraining
  - cases without HPV status
- remodel the vision transformer to be able to handle 3D data
- HPV classification as a downstream task

HELMHOLTZ MUNICH

Results

- extend the public H&N dataset
  - include cases without HPV status info
  - no external testing

HELMHOLTZ MUNICH

Results

- extend the public H&N dataset
  - include cases without HPV status info
  - no external testing
- test set results
  - MAEMI: AUC $= 0.723$
  - C3D: AUC $= 0.710$

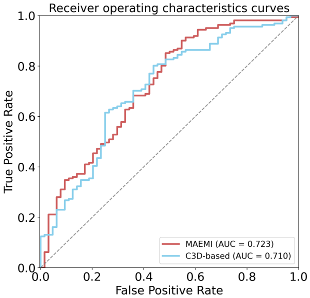

HELMHOLTZ MUNICH

Results

- extend the public H&N dataset
  - include cases without HPV status info
  - no external testing
- test set results
  - MAEMI: AUC $= 0.723$
  - C3D: AUC $= 0.710$
- MAEMI not significantly better
  - small dataset
    - MAEMI: 1k cases
    - C3D: 1M cases
  - optimization limited by computing resources

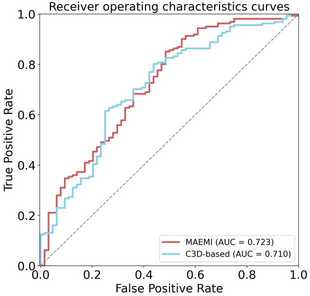

"HPV positive tumors are more radiosensitive"

[1] "HPV, hypoxia and radiation response in head and neck cancer", Göttgens et al., 2018

"HPV positive tumors are more radiosensitive"

- determined *in vitro* via cell survival curves[1]

[1] "HPV, hypoxia and radiation response in head and neck cancer", Göttgens et al., 2018

"HPV positive tumors are more radiosensitive"

- determined *in vitro* via cell survival curves[1]
- on a patient level this is only empirically known

[1] "HPV, hypoxia and radiation response in head and neck cancer", Göttgens et al., 2018

"HPV positive tumors are more radiosensitive"

- determined *in vitro* via cell survival curves[1]
- on a patient level this is only empirically known

→ Survival Analysis

[1] "HPV, hypoxia and radiation response in head and neck cancer", Göttgens et al., 2018

Survival Analysis

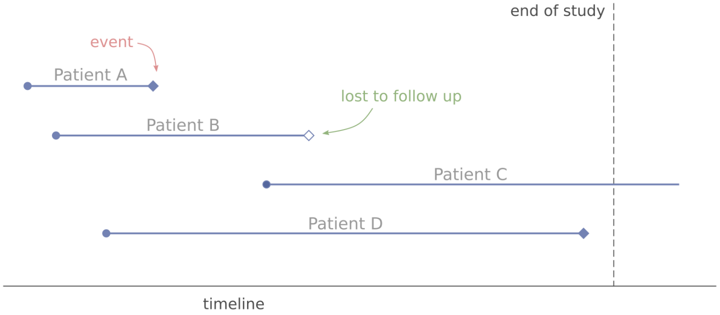

- censoring $\rightarrow$ no simple regression task
- *classical* machine learning $\rightarrow$ Cox model

Survival Analysis

Two most common quantities to model survival are

survival function

$$S(t) = \mathsf{Pr}(T > t), \tag{1}$$

probability to survive beyond time t, event at T

hazard function

$$h(t) = \lim_{\Delta t \to 0} \frac{\mathsf{Pr}(t \leq T < t + \Delta t | T \geq t)}{\Delta t}, \tag{2}$$

momentary rate of occurrence at time t

HELMHOLTZ MUNICH

Cox model

Hazard function for an individual j with covariates $\mathbf{x}_j$:

$$h_j(t|\mathbf{x_j}) = \lambda_0(t) \exp\{\mathbf{x}_j\beta\}, \tag{3}$$

- $\lambda_0(t)$ the baseline hazard function
- $\exp\{\mathbf{x}_j\beta\}$ relative risk associated with $\mathbf{x}_j$

[1] "Regression models and life-tables", Cox, 1972

Cox model

Hazard function for an individual j with covariates $\mathbf{x}_j$:

$$h_j(t|\mathbf{x_j}) = \lambda_0(t)\exp\{\mathbf{x}_j\beta\}, \tag{3}$$

- $\lambda_0(t)$ the baseline hazard function
- $\exp\{\mathbf{x}_j\beta\}$ relative risk associated with $\mathbf{x}_j$

Cox[1] partial likelihood for coefficients β:

$$L(\beta) = \prod_{T_i \text{ uncensored}} \frac{\exp\{\mathbf{x}_i\beta\}}{\sum_{T_j \geq T_i}\exp\{\mathbf{x}_j\beta\}}, \tag{4}$$

[1] "Regression models and life-tables", Cox, 1972

Cox model

Hazard function for an individual j with covariates $\mathbf{x}_j$:

$$h_j(t|\mathbf{x_j}) = \lambda_0(t) \exp\{\mathbf{x}_j \beta\}, \tag{3}$$

- $\lambda_0(t)$ the baseline hazard function
- $\exp\{\mathbf{x}_j \beta\}$ relative risk associated with $\mathbf{x}_j$

Cox[1] partial likelihood for coefficients β:

$$L(\beta) = \prod_{T_i \text{ uncensored}} \frac{\exp\{\mathbf{x}_i \beta\}}{\sum_{T_j \geq T_i} \exp\{\mathbf{x}_j \beta\}}, \tag{4}$$

- Cox could be implemented as a loss in deep learning

[1] "Regression models and life-tables", Cox, 1972

Cox model

Hazard function for an individual j with covariates $\mathbf{x}_j$:

$$h_j(t|\mathbf{x_j}) = \lambda_0(t)\exp\{\mathbf{x}_j\beta\}, \tag{3}$$

- $\lambda_0(t)$ the baseline hazard function
- $\exp\{\mathbf{x}_j\beta\}$ relative risk associated with $\mathbf{x}_j$

Cox[1] partial likelihood for coefficients β:

$$L(\beta) = \prod_{T_i \text{ uncensored}} \frac{\exp\{\mathbf{x}_i\beta\}}{\sum_{T_j \geq T_i}\exp\{\mathbf{x}_j\beta\}}, \tag{4}$$

- Cox could be implemented as a loss in deep learning
- **but** batch wise processing/optimization of weights

[1] "Regression models and life-tables", Cox, 1972

HELMHOLTZ MUNICH

Discrete Survival Model

A scalable discrete-time survival model for neural networks

Michael F. Gensheimer[1] and Balasubramanian Narasimhan[2]

[1] Department of Radiation Oncology, Stanford University, Stanford, CA, United States of America
[2] Department of Statistics, Stanford University, Stanford, CA, United States of America

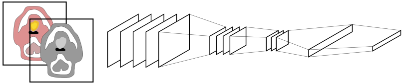

Discrete Survival Model

A scalable discrete-time survival model for neural networks

Michael F. Gensheimer[1] and Balasubramanian Narasimhan[2]

[1] Department of Radiation Oncology, Stanford University, Stanford, CA, United States of America
[2] Department of Statistics, Stanford University, Stanford, CA, United States of America

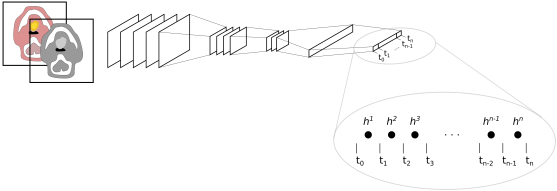

Discrete Survival Model

A scalable discrete-time survival model for neural networks

Michael F. Gensheimer[1] and Balasubramanian Narasimhan[2]

[1] Department of Radiation Oncology, Stanford University, Stanford, CA, United States of America
[2] Department of Statistics, Stanford University, Stanford, CA, United States of America

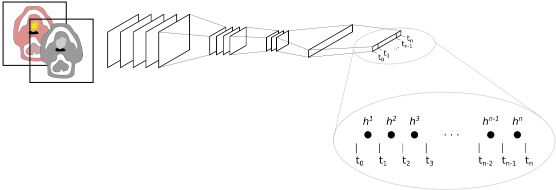

Loss for time interval j:

$$\sum_{i=1}^{d_j} \ln(h_j^i) + \sum_{i=d_j+1}^{r_j} \ln(1 - h_j^i),$$

with

- h^i hazard probability for individual i during j
- r_j individuals not experienced failure or censoring before j
- d_j suffering failure during j

HELMHOLTZ MUNICH

Progression free survival

Task:

- prediction of progression free survival in head and neck cancer

Data:

- PET/CT images for 224 training cases
- 101 test cases
- other clinical patient data

HELMHOLTZ MUNICH

Segmentation

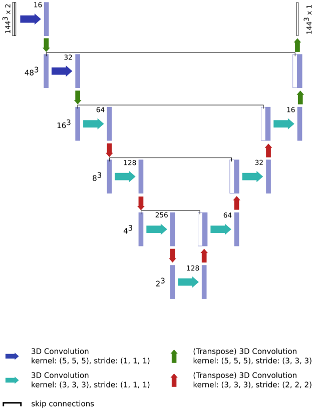

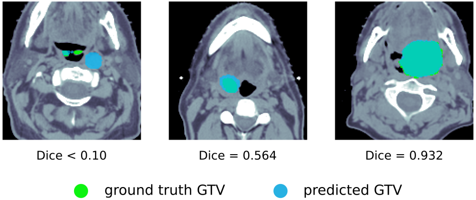

- modified U-Net to fit large 3D volumes

[1] "nnU-Net: Self-adapting framework for U-Net-based medical image segmentation", Isensee et al., 2018

HELMHOLTZ MUNICH

Segmentation

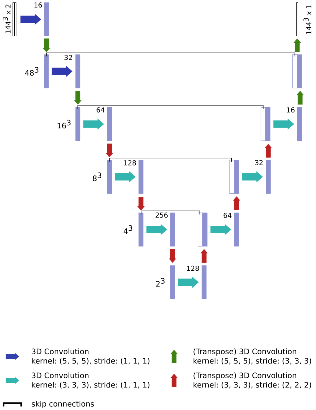

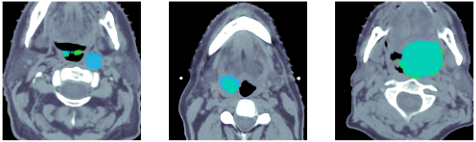

Dice < 0.10 | Dice = 0.564 | Dice = 0.932

ground truth GTV | predicted GTV

- modified U-Net to fit large 3D volumes
- segmentation with DICE of 0.71

$$DSC = \frac{2|A \cap B|}{|A|+|B|}$$

[1] "nnU-Net: Self-adapting framework for U-Net-based medical image segmentation", Isensee et al., 2018

Segmentation

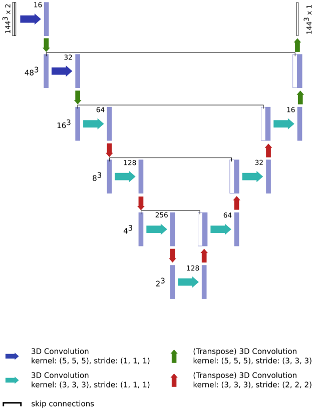

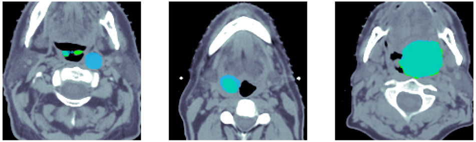

Dice < 0.10 | Dice = 0.564 | Dice = 0.932

ground truth GTV | predicted GTV

- modified U-Net to fit large 3D volumes
- segmentation with DICE of 0.71

$$DSC = \frac{2|A \cap B|}{|A| + |B|}$$

- use the nn-Unet[1]

[1] "nnU-Net: Self-adapting framework for U-Net-based medical image segmentation", Isensee et al., 2018

HELMHOLTZ MUNICH

Survival Model

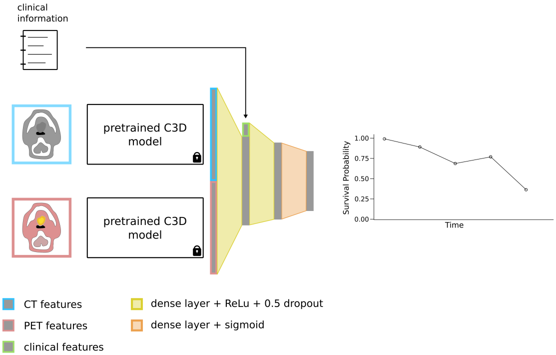

HELMHOLTZ MUNICH

Survival Model

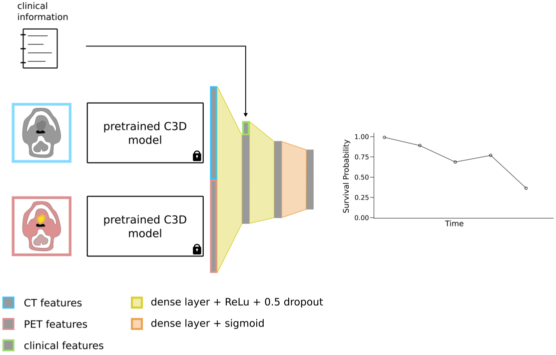

- compute expected time-to-event

$$E(T) = \sum_{k=1}^{n} h^k \prod_{l=0}^{k-1} (1 - h^l)\ t^k, \quad (5)$$

to rank cases (concordance index)

HELMHOLTZ MUNICH

Survival Model

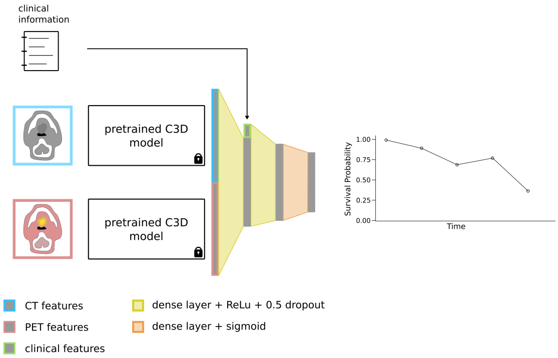

- compute expected time-to-event

$$E(T) = \sum_{k=1}^{n} h^k \prod_{l=0}^{k-1} (1 - h^l)\ t^k, \quad (5)$$

  to rank cases (concordance index)
- patient stratification into subgroups
  - high and low risk cases

HELMHOLTZ MUNICH

Results

	training	validation
c-index	0.899	0.833

Results

	training	validation
c-index	0.899	0.833

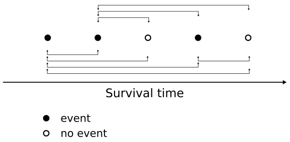

$$\text{c-index} = \frac{\text{pairs of correctly ordered subjects}}{\text{subjects that can actually be ordered}}$$

HELMHOLTZ MUNICH

Results

	training	validation	test
c-index	0.899	0.833	0.668

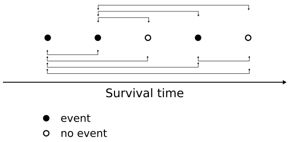

$$\text{c-index} = \frac{\text{pairs of correctly ordered subjects}}{\text{subjects that can actually be ordered}}$$

HELMHOLTZ MUNICH

Results

	training	validation	test
c-index	0.899	0.833	0.668

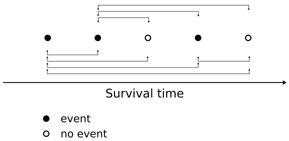

$$\text{c-index} = \frac{\text{pairs of correctly ordered subjects}}{\text{subjects that can actually be ordered}}$$

- considerable drop between train/validation and test set
  - small dataset $\rightarrow$ overfitting
  - partial external testing

  $\rightarrow$ larger dataset needed
- a perfect model would be suspicious

Results

	training	validation	test
c-index	0.899	0.833	0.668

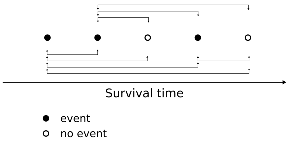

$$\text{c-index} = \frac{\text{pairs of correctly ordered subjects}}{\text{subjects that can actually be ordered}}$$

- considerable drop between train/validation and test set
  - small dataset → overfitting
  - partial external testing

  → larger dataset needed
- a perfect model would be suspicious
  - no treatment information included

Anomaly detection

Unsupervised anomaly detection

train model to detect any kind of divergence from normal/healthy examples

Unsupervised anomaly detection

train model to detect any kind of divergence from normal/healthy examples

Training

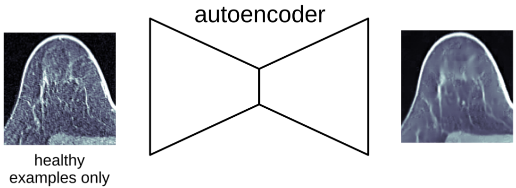

Unsupervised anomaly detection

train model to detect any kind of divergence from normal/healthy examples

Training

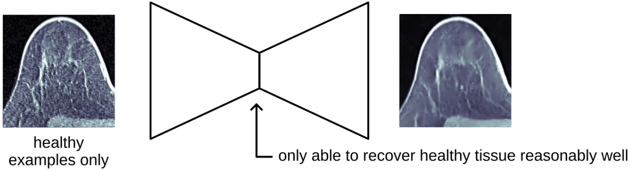

Unsupervised anomaly detection

train model to detect any kind of divergence from normal/healthy examples

Inference

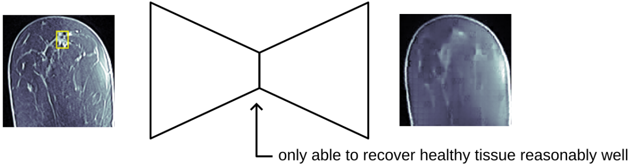

Unsupervised anomaly detection

train model to detect any kind of divergence from normal/healthy examples

Inference

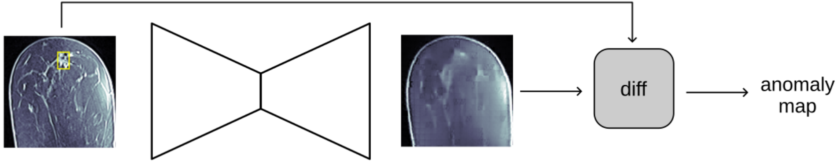

Breast cancer anomaly detection

- mammography depicts the standard breast cancer screening technique
- **but** features
  - susceptibility to **overdiagnosis**
  - **low sensitivity** in dense tissue

Breast cancer anomaly detection

- mammography depicts the standard breast cancer screening technique
- **but** features
  - susceptibility to **overdiagnosis**
  - **low sensitivity** in dense tissue
- dynamic contrast enhanced (DCE)-MRI features higher sensitivity

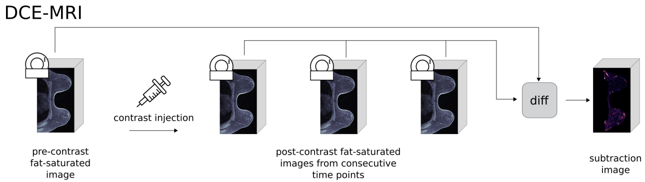

HELMHOLTZ MUNICH

Breast cancer anomaly detection

- mammography depicts the standard breast cancer screening technique
- **but** features
  - susceptibility to **overdiagnosis**
  - **low sensitivity** in dense tissue
- dynamic contrast enhanced (DCE)-MRI features higher sensitivity

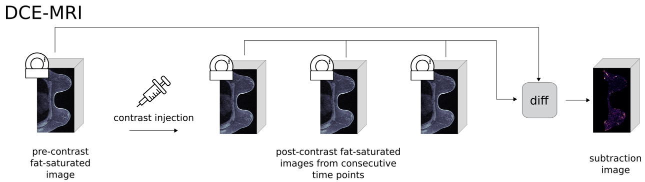

- **but** comes with: long scan times - high costs - contrast agent - motion artifacts

Breast cancer anomaly detection

- mammography depicts the standard breast cancer screening technique
- **but** features
  - susceptibility to **overdiagnosis**
  - **low sensitivity** in dense tissue
- dynamic contrast enhanced (DCE)-MRI features higher sensitivity

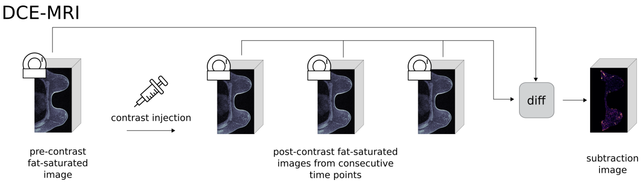

- **but** comes with: long scan times - high costs - contrast agent - motion artifacts

→ anomaly detection models may have the power to overcome those limitations?

Breast cancer anomaly detection

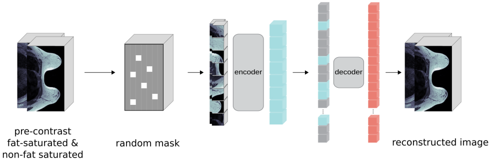

HELMHOLTZ MUNICH

Breast cancer anomaly detection

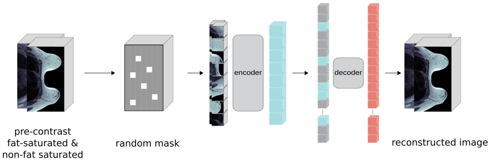

- masked autoencoder for anomaly detection

Breast cancer anomaly detection

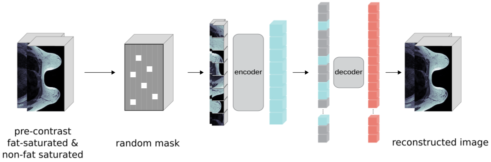

- masked autoencoder for anomaly detection
- train on healthy **non-contrast** enhanced breast cancer MRI

HELMHOLTZ MUNICH

Breast cancer anomaly detection

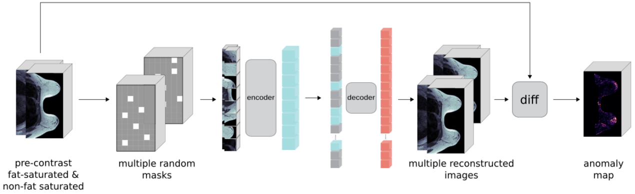

- masked autoencoder for anomaly detection
- train on healthy **non-contrast** enhanced breast cancer MRI
- during inference:
  - introduce multiple random masks $\longrightarrow$ probability to mask anomaly
  - use complete autoencoder structure

HELMHOLTZ MUNICH

Breast cancer anomaly detection

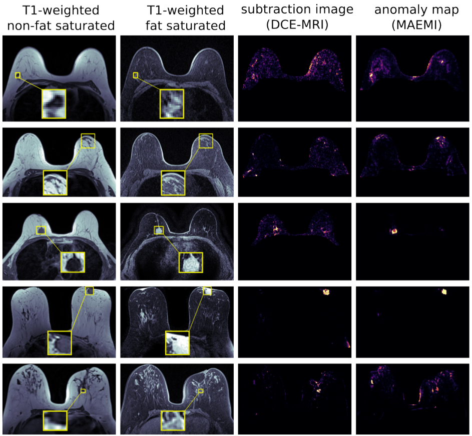

HELMHOLTZ MUNICH

Breast cancer anomaly detection

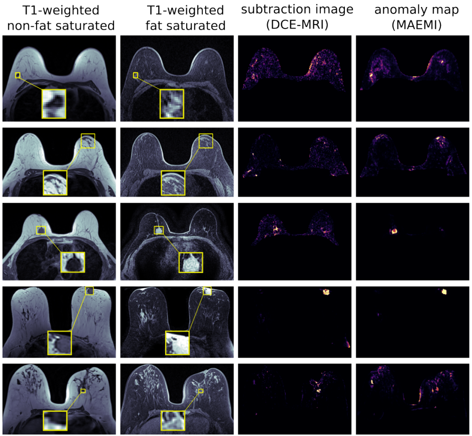

	AUROC	AP
MAEMI	**0.732**	0.081
DCE-MRI	0.705	**0.127**

HELMHOLTZ MUNICH

Breast cancer anomaly detection

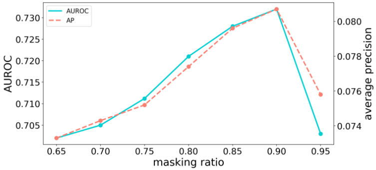

Breast cancer anomaly detection

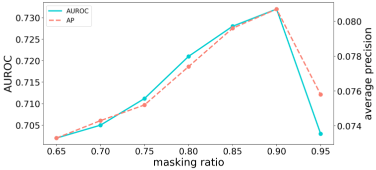

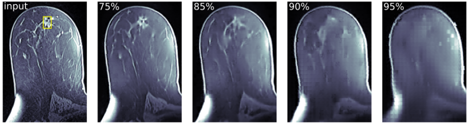

Breast cancer anomaly detection

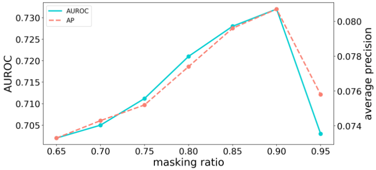

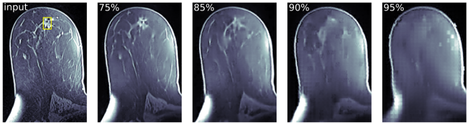

Future work:

- train/test on larger external dataset
- further validation with radiologists

Reconstruction of pseudo-health examples

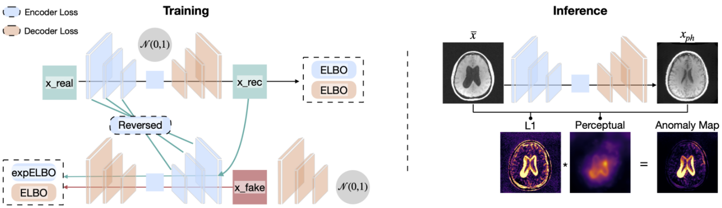

"Generalizing Unsupervised Anomaly Detection: Towards Unbiased Pathology Screening", Bercea et al., 2023

Reconstruction of pseudo-health examples

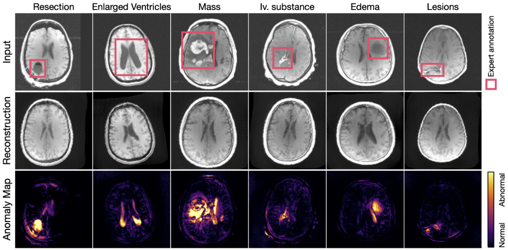

"Generalizing Unsupervised Anomaly Detection: Towards Unbiased Pathology Screening", Bercea et al., 2023

HELMHOLTZ MUNICH

Reconstruction of pseudo-health examples

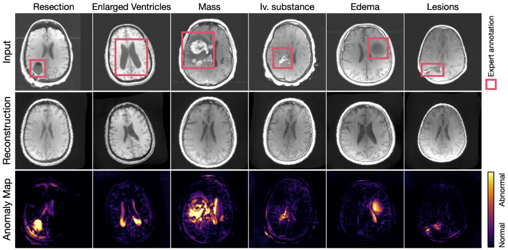

Current limitations:

- bounding boxes as ground truth labels
- no healthy examples

"Generalizing Unsupervised Anomaly Detection: Towards Unbiased Pathology Screening", Bercea et al., 2023

Thank you!

lang@helmholtz-munich.de

langdaniel

Liu, Changxing et al. "The molecular mechanisms of increased radiosensitivity of HPV-positive OPSCC". In: *Journal of Otolaryngology-Head & Neck Surgery* 47.1 (2018), pp. 1–8 (cit. on pp. 12, 13).

Maniakas, Anastasios et al. "North-American survey on HPV-DNA and p16 testing for head and neck squamous cell carcinoma". In: *Oral oncology* 50.10 (2014), pp. 942–946 (cit. on pp. 12, 13).

Tran, Du et al. "Learning spatiotemporal features with 3d convolutional networks". In: *Proceedings of the IEEE international conference on computer vision*. 2015, pp. 4489–4497 (cit. on pp. 18–20).

Lang, Daniel M et al. "Deep learning based HPV status prediction for oropharyngeal cancer patients". In: *Cancers* 13.4 (2021), p. 786 (cit. on p. 21).

Göttgens, Eva-Leonne et al. "HPV, hypoxia and radiation response in head and neck cancer". In: *The British journal of radiology* 92.1093 (2018), p. 20180047 (cit. on pp. 37–40).

Cox, David R. "Regression models and life-tables". In: *Journal of the Royal Statistical Society: Series B (Methodological)* 34.2 (1972), pp. 187–202 (cit. on pp. 43–46).

Isensee, Fabian et al. "nnU-Net: Self-adapting framework for U-Net-based medical image segmentation". In: *arXiv preprint arXiv:1809.10486* (2018) (cit. on pp. 51–53).

Bercea, Cosmin I et al. "Generalizing Unsupervised Anomaly Detection: Towards Unbiased Pathology Screening". In: *Medical Imaging with Deep Learning*. 2023 (cit. on pp. 81–83).